



Preparation of Cellulose Acetate Nanocomposite Films Based on TiO₂-ZnO Nanoparticles Modification as Food Packaging Applications

^{1,2}Hajer A. Ali, ²Nahida J. Hameed*

¹Mesopotamian State Company of Seeds, Ministry of Agriculture – Iraq

²Materials Science Division, Department of Applied Sciences, University of Technology – Iraq

Article information

Article history:

Received: December, 18, 2021

Accepted: April, 02, 2022

Available online: September, 10, 2022

Keywords:

Antibacterial activity,
Biodegradable,
Contact angle,
Mechanical properties

*Corresponding Author:

Nahida J. Hameed

nahidajoumaa61@yahoo.com

Abstract

To develop bio-packaging materials, nanocomposite films of cellulose acetate reinforced with titanium dioxide and zinc oxide nanoparticles were prepared, by the casting method at different weight ratios of ZnO nanoparticles (1.5, 2, and 2.5) wt% and a constant weight ratio of 2 wt% TiO₂. ZnO and TiO₂ nanoparticles were tested using scanning electron microscopy (SEM). The mechanical properties (tensile strength and elongation) were improved at a fixed level of Cellulose Acetate+ 2% TiO₂+1.5wt% ZnO loading. Beyond that level of loading, they decreased. The tensile strength was decreased due to some degrees of agglomeration of filler particles above a critical content. Fourier-Transform Infrared Spectroscopy (FTIR) was conducted to reveal the microstructures and chemical composition of as-prepared composite films. The wettability of the films was also determined by the sessile drop method. An increase in contact angle was also observed by the addition of ZnO content from 70.6° to 77.1° compared to pure Cellulose Acetate, which indicated a value of 61.3°. Antibacterial activity against Escherichia coli and Staphylococcus aureus was enhanced after incorporation of ZnO-TiO₂ compared with pure CA. The enhanced wettability and antibacterial activity of the prepared films suggest that they could be used for packaging applications.

DOI: [10.53293/jasn.2022.4542.1122](https://doi.org/10.53293/jasn.2022.4542.1122), Department of Applied Sciences, University of Technology
This is an open access article under the CC BY 4.0 License.

1. Introduction

Food packaging and contact surfaces with food have been a cause of worry in the food industry since they do not provide enough protection or maintain the freshness of products. However, the possibility of extending the shelf life of foods via microbial resistance as well as lowering the growth rate of bacteria has been a focus of academic and corporate research. Packaging technology offers limitless possibilities for food preservation, and Cellulose Acetate (CA), which is made from naturally occurring cellulose materials such as wood, cotton, and rice husk, is a green product that has been nominated for use in the creation of food packaging films. It is favored for its superior appearance, biodegradability, greater durability, and nontoxicity [1-3]. It is applied in several ways, including filters, medication delivery, and medical implants [4-7]. Due to their edible, renewable, and

biodegradable qualities, biopolymer-based films have been often used in packaging [8-12]. To increase the functionality of packaging, nanoparticles such as zinc oxide and titanium dioxide have been used to create composite functional films [13, 14]. Because of their stability, ability to suppress bacterial growth, and ability to prevent the formation of new cell structures, TiO₂ nanoparticles have gained substantial attention [15]. These nanoparticles have improved mechanical capabilities, which are stable under hard circumstances, and are antibacterial owing to the active oxygen species formed by metal oxide particles [16]. The US Food and Drug Administration (USFDA) has approved the use of TiO₂ and ZnO nanoparticles as food additives and food contact chemicals after undertaking a safety investigation [17, 18]. The insertion of nanoparticles such as zinc oxide (ZnO) and titanium dioxide (TiO₂) nanostructures into cellulose acetate has been suggested to remove dithioerethiol (DTT) from water and to be utilized as a covering for wood preservation [19-21]. Nanocomposites of cellulose acetate based on Au/ZnO showed a greater water contact angle and increased photocatalytic activity than pure cellulose acetate [22, 23]. Additionally, it has been demonstrated that black grapefruits with ZnO-incorporated cellulose acetate phthalate and chitosan have a longer shelf life [24]. The current study focuses on the synthesis and application of cellulose acetate thick films that combine ZnO-TiO₂ nanoparticles. It is different from previous studies in that it incorporates different materials and conducts various examinations for food packaging applications. The physical and chemical properties of the ZnO-TiO₂ nanocomposite films, as well as their antibacterial activity and contact angle, are investigated.

2. Experimental Procedure

2.1. Materials

CA (CDH India, acetyl content 29-45%; Maximum limit of impurities; 0.1%; free acid (as acetic acid); 5.0%; loss on drying at 105°C sulphated ash; 0.1%) and Acetone AR/ACS (2-Propanone, Dimethylketone) (M.W.:58.08) from (CDH India). Titanium oxide nanoparticles/nanopowder (TiO₂, Rutile, 99.5%), particle size (20-40) nm, Zinc Oxide nanoparticles (99.8%), particle size (20-50) was purchased from (Skyspring, USA).

2.2. Methodology

2.2.1. Preparation of primary polymer solutions

The main solution of CA was made using the casting technique by dissolving 7 g of CA in 100 ml of acetone. After 8 hours of stirring with a magnetic stirrer, the solution was cast on a glass petri dish, and a final film was achieved after 48 hours.

2.2.2 Preparation of ZnO/TiO₂/CA composite polymer solution

ZnO and TiO₂ nanoparticles with C₃H₆O Solution were added to CA Powder at a different weight ratio of ZnO nanoparticle (1.5, 2, and 2.5 wt.%) and a constant weight ratio of 2% TiO₂ of the composite film. The mixture was stirred until getting the homogeneous solutions; Then the solution was cast in a glass Petri dish and left to dry for 48 hrs. The preparation process was shown in Figure 1.

2.3. Characterization

The morphology of the powder was examined with (FESEM Zeiss Sigma 300-HV Germany). The mechanical characteristics of the cellulose acetate and the composite's thick films were measured by tensile tests using Laryee Universal Testing Machine (UTM) UE3450 from (Laryee Technology Co., Ltd. China). The films were cut to 120 mm × 10 mm, and the thickness was measured by a digital micrometre with ±1 μm accuracy. All the tests were performed at room temperature (around 27°C) and a crosshead speed of 5 mm/min. was used during the measurements of the cellulose-based films, and a stress-strain curve was recorded. Young's modulus, elongation at the breakpoint, and ultimate tensile strength were determined using the equation below [25]:

$$\text{Young modulus (Mpa)} = \text{Stress (Mpa)} / \text{Strain} \quad (1)$$

$$\text{Strees (Mpa)} = \text{Force (N)} / \text{Area (mm}_2) \quad (2)$$

$$\text{Strain} = \text{Elongation (\%)} = \Delta L / L_0 * 100\% \quad (3)$$

$$\Delta L \text{ (mm)} = L_1 - L_0 \text{ (mm)} \quad (4)$$

Where ΔL : is the amount of the change that occurs in length, L_1 : is the length after the deformation, L_0 is the original length.

$$\text{Ultimate tensile strength (Mpa)} = P_{\max} \text{ (N)} / A \text{ (mm}_2) \quad (5)$$

Where P_{\max} : Maximum tensile load a sample can withstand during the test, A is the Area. Fourier transformed infrared (FTIR) spectra were obtained by (SHIMADZU-8400S FTIR spectrometer, Japan). The spectra were obtained in the wavenumber range of $400\text{-}4000 \text{ cm}^{-1}$, 4 cm^{-1} resolutions. The samples were prepared as tablets by mixing with KBr powder.

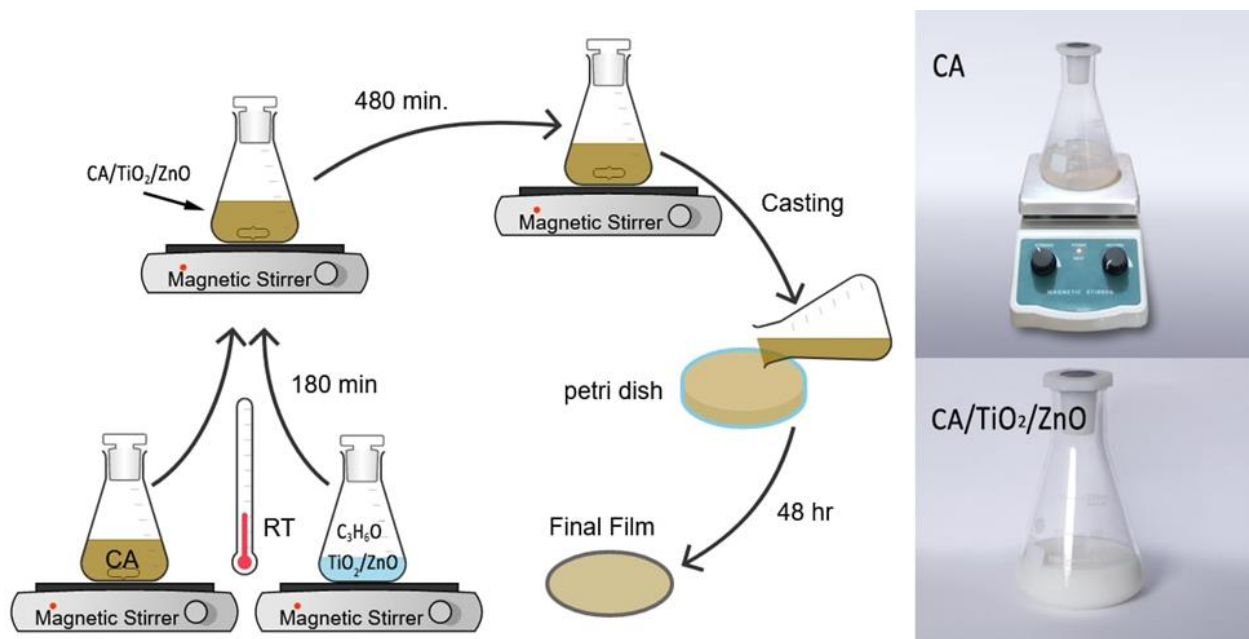


Figure 1: A schematic diagram of the preparation process for the films, on the right, the device used to prepare the compound (CA) and the final solution of the films (CA/TiO₂/ZnO).

The optical system used to measure contact angle was from (Holmarc Opto-Mechatronics P Ltd. India), with an automated dispenser and software for static and dynamic contact angle measurement. A drop of water is placed on the film surface and it will spread on the surface based on the interactions between the solid surface and the water. Water contact angle will be measured to indicate the wettability of the surface. The antibacterial activity of the CA and CA/TiO₂/ZnO was tested against human pathogens *Escherichia coli* and *Staphylococcus aureus* using the following protocol. The bacteria were captured from their stock cultures using a sterile wire loop. To assess how CA and CA/TiO₂/ZnO have an impact on the bacteria's growth curve, the bacterial strains were grown at 37° C on M-H agar plates with inoculations of 50 mL of nutrient broth. The bacterial growth grew until the nutritional broth attained an optical density (OD) of 0.1 at 600 nm, which corresponds to a bacterial concentration

of 108 CFU/mL. The bacterial cultures (1 mL) were then added to the nutritional broth along with CA and CA/TiO₂/ZnO, and incubated at 37°C for 12 hours with slight agitation. The OD was measured with a spectrophotometer to determine bacterial growth. An unpaired t-test was used to statistically assess the obtained data. The results were provided as the mean ± SD of triplicate measurements.

3. Results and Discussion

3.1. SEM Analysis

SEM micrographs of TiO₂ and ZnO powders are shown in Figure 2. As demonstrated, TiO₂ and ZnO nanopowders have extremely small particle sizes with a narrow particle size distribution of around 20-40nm and 20-50nm, respectively. Due to the increased surface area of fine particles, a more complex dispersion approach will be necessary to avoid agglomeration and to provide a more homogeneous particle size distribution within the CA matrix.

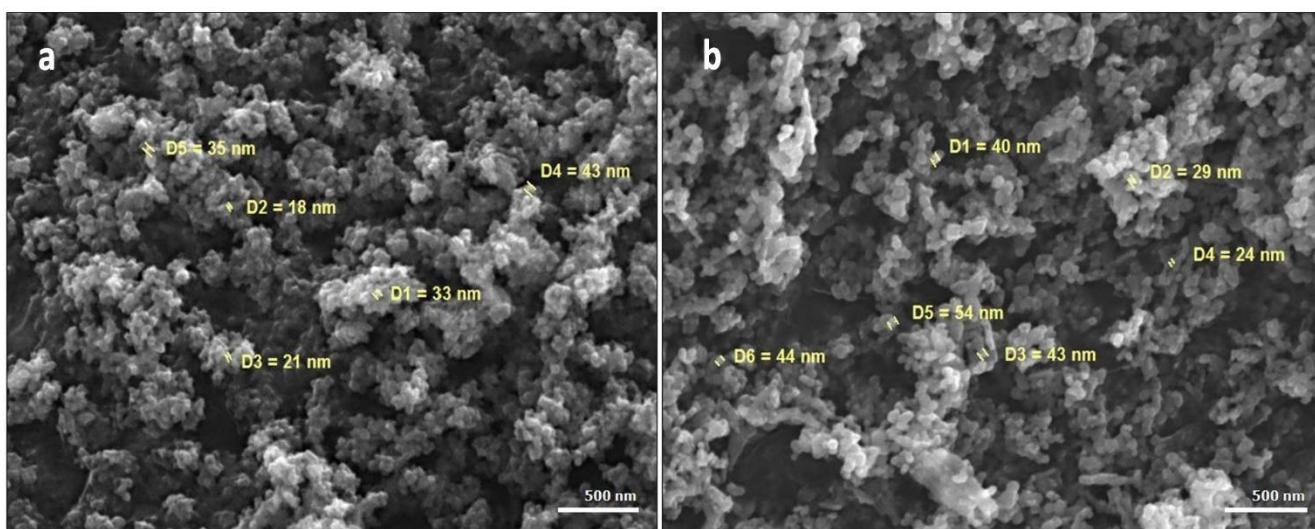


Figure 2: SEM images of (a) TiO₂ nanoparticle, (b) ZnO nanoparticle.

4.2. Tensile Test

As shown in Figure 3, the stress-strain curves for ZnO-TiO₂ /CA composite films were obtained using varied weight ratios of ZnO nanoparticles (1.5, 2, and 2.5%) in addition to a constant weight ratio of 2 wt% TiO₂ in the composite film.

Improved mechanical characteristics were seen when inorganic fillers were distributed evenly throughout the (CA) polymer matrix, with up to 1.5 weight percent zinc oxide and 2 weight percent titanium dioxide being used. Significant parameters were taken from Figure 3 and displayed in Figures 4, and 5, demonstrating their variation with ZnO concentrations [26-28].

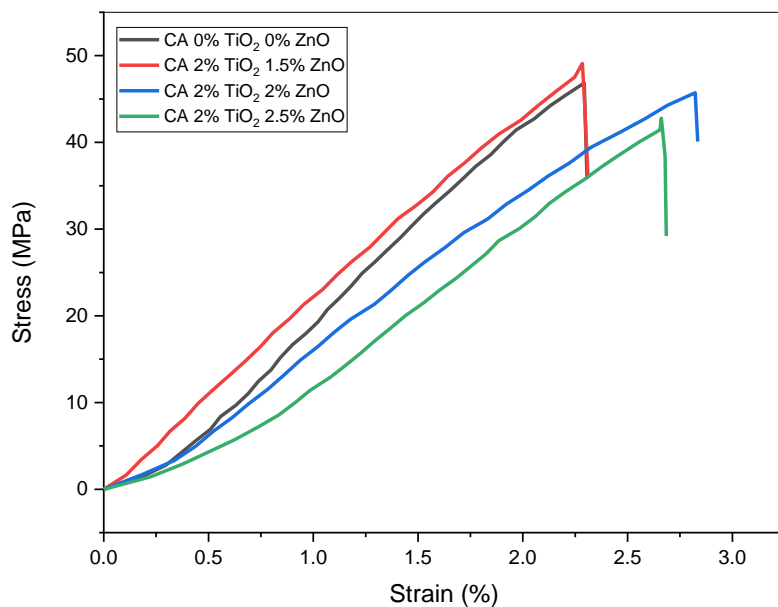


Figure 3: The stress-strain curve of ZnO/TiO₂ with Cellulose acetate.

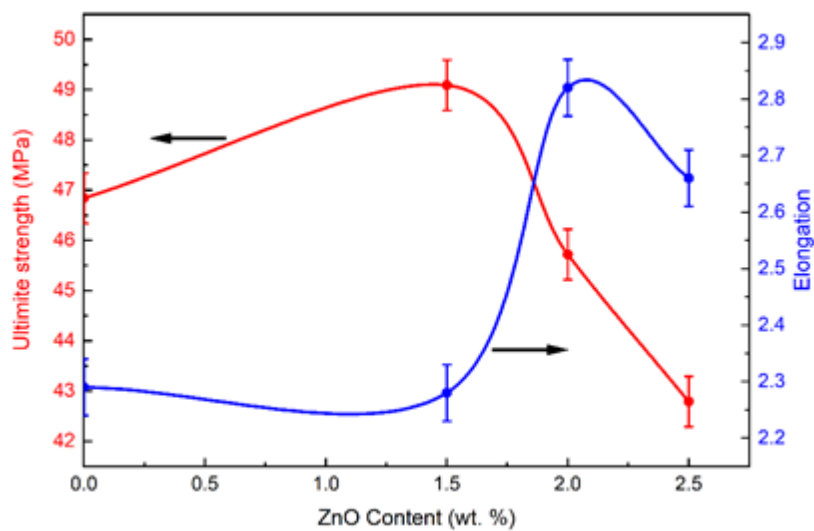


Figure 4: Variation of the ultimate tensile strength and elongation of CA/TiO₂ films with different ZnO content.

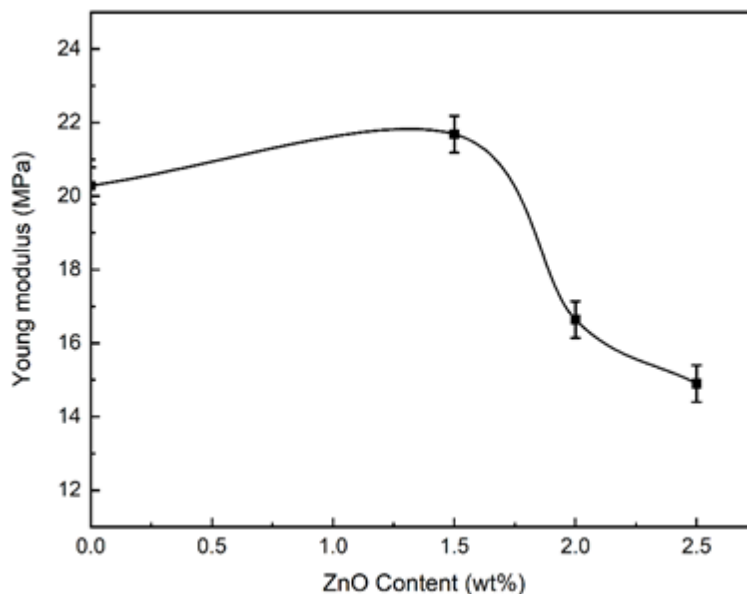


Figure 5: Young modulus of Cellulose acetate and TiO₂ films with different ZnO content.

The intermolecular force chain, stiffness, and molecular symmetry of polymer systems all influence the mechanical characteristics of polymer systems [29]. Polymers with a high degree of crystallinity, crosslinking, or rigid chains have high strength or limited extensibility, resulting in a high yield modulus, high stress at peak value, and a low elongation value. Because of electrostatic interactions between the ester atoms of one chain and the hydroxyl group of another, CA is a stiff and strong material that shows dipole-dipole attraction between the two chains. The interaction of dipole-dipole attraction, which achieves its greatest magnitude, was shown to relate to an improvement in the mechanical properties of materials. A significant increase in the filler's ability to cling to the matrix was associated with a decrease in the amount of sliding between the composite layers when stress was applied to the composites [30, 31]. The tensile strength is reduced due to some degrees of agglomeration of filler particles above the critical content and an increase in inhomogeneity [27, 28]. The lack of interfacial adhesion between the polymer and the fillers was responsible for the decrease in tensile strength [31]. At a fixed level of 1.5% ZnO- 2% TiO₂/CA loading; both tensile strength and elongation were improved as shown in Figure 4, beyond that level of loading the values of tensile strength and elongation decreased. The general behaviour of the Young's modulus was found to be dependent on the elongation and ultimate strength according to the filler contents and the homogeneity of particle distribution within the CA matrix.

4.3. FTIR Spectroscopy

Figure 6 showed FTIR spectra of pure CA film and CA films containing different weight ratios of ZnO nanoparticle (1.5, 2, and 2.5) wt% and a constant weight ratio of 2 wt% TiO₂. The film spectrum is characterized by the presence of bands at 1741 cm⁻¹ (steric carbonyl stretching), 3478 cm⁻¹ (cellulose OH stretching), and 2936 cm⁻¹ (CH stretching) [32]. The bands of 2936 cm⁻¹ (CH stretching), 3478 cm⁻¹ (OH stretching), 1741 cm⁻¹ (steric carbonyl stretching), 1232 cm⁻¹, and 1045 cm⁻¹ (C-O stretching), all increased when ZnO-TiO₂ nanoparticle were added. Because TiO₂ is an oxide with O-Ti-O bonding in its chemical structure, inserting it into cellulose acetate may have increased the interactions between the two compounds at the region of the band that represented these properties. TiO₂ bonding is represented by peaks at 600 cm⁻¹ and 750 cm⁻¹ [33, 34]. Carbonian and hydroxyl groups have peaks centered at 1750 cm⁻¹ and 3478 cm⁻¹, respectively [32]. The vibration frequency of O-Zn-O bond groups is indicated by the peak at 400-600 cm⁻¹ [24].

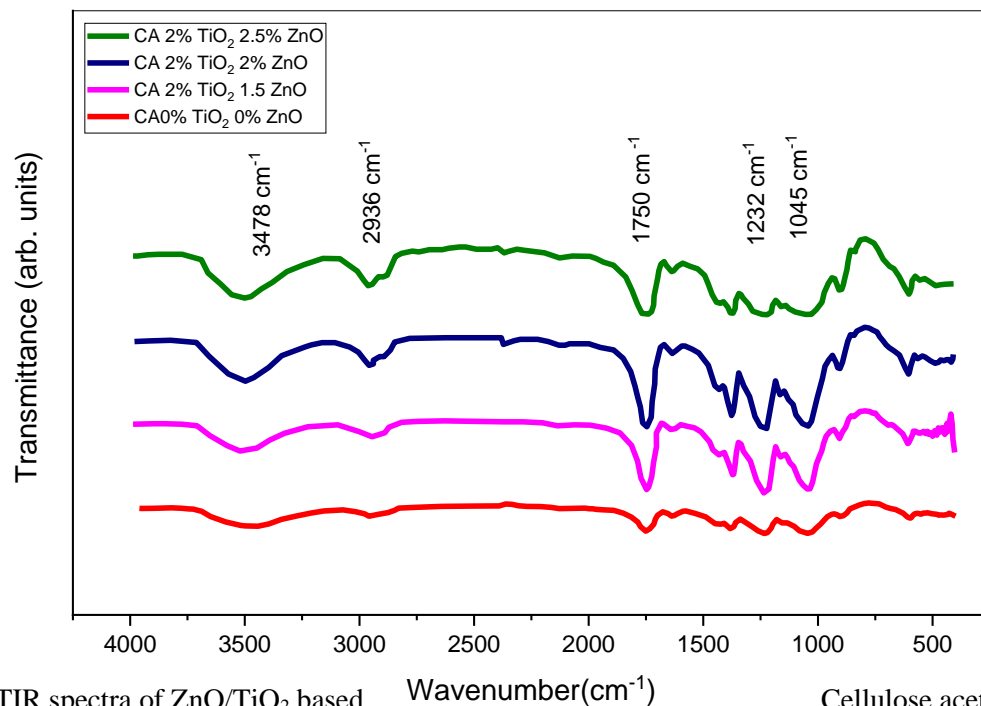


Figure 6: FTIR spectra of ZnO/TiO₂ based Cellulose acetate.

4.4. Water Contact Angle

Wettability testing measures how many water molecules a sample can absorb in a certain period. The wettability character of a surface is described as whether or not the sample is hydrophilic or hydrophobic, in general. Figure 7 depicts the water contact angles for CA and ZnO-TiO₂/CA at varied weight ratios of ZnO nanoparticle (1.5, 2, and 2.5) wt % and a constant weight ratio of 2 wt% TiO₂. Its hydrophilic nature resulted in a contact angle of 61.3° for the CA film, which was the lowest of all the films tested. Low surface wettability leads to a high contact angle and vice versa [35], hence the CA film had the lowest surface wettability of all the films tested. When compared to CA film, all-composite films had greater contact angles of 70.6°, 72.9°, and 77.1°, respectively. The contact angle of the produced films increased in the direction of hydrophobicity as the amount of nano ZnO present in them increased [22].

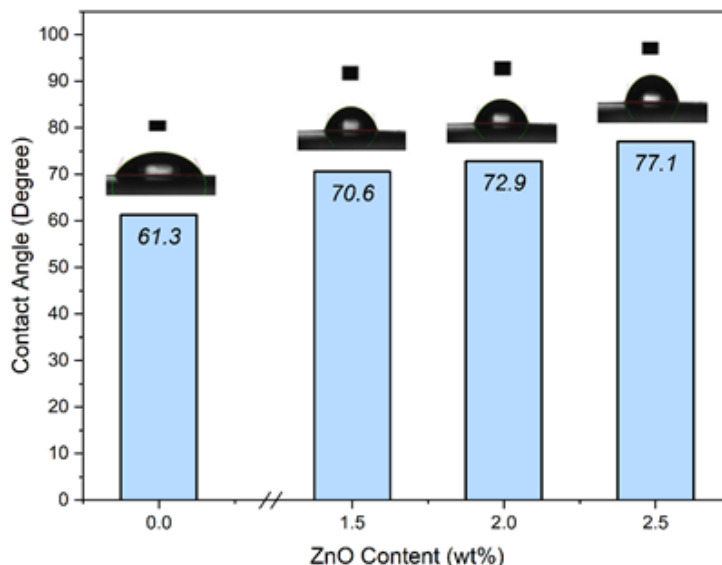


Figure 7: water contact angle for CA film and nanocomposite thick films with various ZnO content. The inset pictures show the images for the measurement of surface contact angles

4.5 Antibacterial Activity

The Optical Density (OD) of *Escherichia coli* and *Staphylococcus aureus* suspensions at 600 nm treated with different films in test tubes for 12 hours was measured, which is a commonly used method for determining the growth of bacteria for the assessment of antibacterial activities [36, 37]. In general, the lower the optical density of bacteria suspension at 600 nm after a specific period of cultivation, the better the antibacterial film's activity. As shown in Table 1, the OD₆₀₀ values for various antibacterial films were in the following order: control > CA > CA/2% TiO₂/1.5% ZnO > CA/2% TiO₂/2% ZnO > CA/2% TiO₂/2.5% ZnO. It is important to note that the nanocomposite film made up of CA+2% TiO₂+2.5% ZnO had the lowest OD₆₀₀. In contrast to other antibacterial films, this film performed particularly well after 12 hours of cultivation. These results clearly showed that TiO₂ and ZnO have a greater ability to resist bacteria growth [38-43].

Table 1. Effect of CA and CA/TiO₂/ZnO in *E. coli* and *S. aureus* growth curve.

Film Code	TiO ₂ wt%	ZnO wt%	Optical Density (OD) @600nm	
			<i>E. coli</i>	<i>S. aureus</i>
Control	-	-	0.62 ± 0.05	0.58 ± 0.04
CA000	0.0	0.0	0.53 ± 0.03606	0.46 ± 0.06
CA215	2.0	1.5	0.16 ± 0.03055	0.19 ± 0.02517
CA220	2.0	2.0	0.14 ± 0.02082	0.14 ± 0.01528
CA225	2.0	2.5	0.13 ± 0.02	0.12 ± 0.00577

The results are means of three replicates; ±, standard deviation (SD).

3. Conclusion

The present work employed the casting process to make ZnO-TiO₂/CA composite films, which were then characterized. The tensile test demonstrated that the ultimate tensile strength and elongation were increased at a fixed loading level of 1.5 percent ZnO-2 percent TiO₂/CA; however, once the loading level was exceeded, the values of tensile strength and elongation began to decline. The interaction between CA and ZnO-TiO₂ was established by their FTIR spectra. The inclusion of ZnO resulted in an increase in hydrophobicity, which was also observed. When compared to pure CA, the combination of CA/TiO₂/ZnO exhibits increased antibacterial activity

against *Escherichia coli* and *Staphylococcus aureus*. Because of the wettability characteristics and antibacterial activity of the produced films, they have the potential to be employed in packaging applications.

Acknowledgment

The authors express their appreciation to Ali J. Addie, Mukhallad H. Shwaish, Dr. Mohammed S. Ali, Dr. Hanaa J. Kadhim, Dr. M.S. Jabir for their help in Examinations and our appreciation to all staff of the Journal.

Conflict of Interest

The authors declare that they have no conflict of interest.

Reference

- [1] Sharma, S. K. Giri, K. P. R. Kartha, and R. S. Sangwan, "Value-additive utilization of agro-biomass: preparation of cellulose triacetate directly from rice straw as well as other cellulosic materials," *RSC Adv.*, vol. 7, no. 21, pp. 12745–12752, 2017.
- [2] R. G. Candido, G. G. Godoy, and A. Gonçalves, "Characterization and application of cellulose acetate synthesized from sugarcane bagasse," *Carbohydr. Polym.*, vol. 167, pp. 280–289, 2017.
- [3] E. Samios, R. K. Dart, and J. V. Dawkins, "Preparation, characterization and biodegradation studies on cellulose acetates with varying degrees of substitution," *Polymer*, vol. 38, no. 12, pp. 3045–3054, 1997.
- [4] A. T. Holkem *et al.*, "Development and characterization of alginate microcapsules containing *Bifidobacterium* BB-12 produced by emulsification/internal gelation followed by freeze drying," *LWT - Food Science and Technology*, vol. 71, pp. 302–308, 2016.
- [5] J. Li, J. He, Y. Huang, D. Li, and X. Chen, "Improving surface and mechanical properties of alginate films by using ethanol as a co-solvent during external gelation," *Carbohydrate Polymers*, vol. 123, pp. 208–216, 2015.
- [6] S. Sarkar, S. Chakraborty, and C. Bhattacharjee, "Photocatalytic degradation of pharmaceutical wastes by alginate supported TiO₂ nanoparticles in packed bed photo reactor (PBPR)," *Ecotoxicology and Environmental Safety*, vol. 121, pp. 263–270, 2015.
- [7] H.-M. D. Wang, C.-C. Chen, P. Huynh, and J.-S. Chang, "Exploring the potential of using algae in cosmetics.," *Bioresour. Technol.*, vol. 184, pp. 355–362, May 2015.
- [8] T. de Moraes Crizel, A. de Oliveira Rios, V. D. Alves, N. Bandarra, M. Moldão-Martins, and S. Hickmann Flôres, "Biodegradable Films Based on Gelatin and Papaya Peel Microparticles with Antioxidant Properties," *Food Bioprocess Technol.*, vol. 11, no. 3, pp. 536–550, 2018.
- [9] Y. A. Arfat, M. Ejaz, H. Jacob, and J. Ahmed, "Deciphering the potential of guar gum/Ag-Cu nanocomposite films as an active food packaging material.," *Carbohydr. Polym.*, vol. 157, pp. 65–71, Feb. 2017.
- [10] Z. Wang, J. Narciso, A. Biotteau, A. Plotto, E. Baldwin, and J. Bai, "Improving Storability of Fresh Strawberries with Controlled Release Chlorine Dioxide in Perforated Clamshell Packaging," *Food Bioprocess Technol.*, vol. 7, no. 12, pp. 3516–3524, 2014.
- [11] C. V. L. Giosafatto, P. Di Pierro, A. P. Gunning, A. MacKie, R. Porta, and L. Mariniello, "Trehalose-containing hydrocolloid edible films prepared in the presence of transglutaminase," *Biopolymers*, vol. 101, no. 9, pp. 931–937, 2014.
- [12] Z. Feng, G. Wu, C. Liu, D. Li, B. Jiang, and X. Zhang, "Edible coating based on whey protein isolate nanofibrils for antioxidation and inhibition of product browning," *Food Hydrocolloids*, vol. 79, pp. 179–188, 2018.
- [13] H. Chen, J. N. Seiber, and M. Hotze, "ACS select on nanotechnology in food and agriculture: A perspective on implications and applications," *Journal of Agricultural and Food Chemistry*, vol. 62, no. 6, pp. 1209–1212, 2014.

- [14] A. Sturaro, R. Rella, G. Parvoli, D. Ferrara, and F. Tisato, "Contamination of dry foods with trimethyldiphenylmethanes by migration from recycled paper and board packaging," *Food Addit. Contam.*, vol. 23, no. 4, pp. 431–436, 2006.
- [15] V. Goudarzi and I. Shahabi-Ghahfarrokhi, "Photo-producible and photo-degradable starch/TiO₂ bionanocomposite as a food packaging material: Development and characterization," *International Journal of Biological Macromolecules*, vol. 106, pp. 661–669, 2018.
- [16] C. Pittarate, T. Yoovidhya, W. Srichumpuang, N. Intasanta, and S. Wongsasulak, "Effects of poly(ethylene oxide) and ZnO nanoparticles on the morphology, tensile and thermal properties of cellulose acetate nanocomposite fibrous film," *Polym. J.*, vol. 43, no. 12, pp. 978–986, 2011.
- [17] S. Tang *et al.*, "Degradable and photocatalytic antibacterial Au-TiO₂/sodium alginate nanocomposite films for active food packaging," *Nanomaterials*, vol. 8, no. 11, 2018.
- [18] C. Pittarate, T. Yoovidhya, W. Srichumpuang, N. Intasanta, and S. Wongsasulak, "Effects of poly(ethylene oxide) and ZnO nanoparticles on the morphology, tensile and thermal properties of cellulose acetate nanocomposite fibrous film," *Polym. J.*, vol. 43, no. 12, pp. 978–986, 2011.
- [19] Z. Alhalili, C. Romdhani, H. Chemingui, and M. Smiri, "Removal of dithioerethiol (DTT) from water by membranes of cellulose acetate (AC) and AC doped ZnO and TiO₂ nanoparticles," *J. Saudi Chem. Soc.*, vol. 25, no. 8, p. 101282, 2021.
- [20] M. E. David, R.-M. Ion, E. R. Andrei, R. M. Grigorescu, L. Iancu, and M. I. Filipescu, "Superhydrophobic Coatings Based on Cellulose Acetate for Superhydrophobic Coatings Based on Cellulose Acetate for Pinewood Preservation," *J. Sci. Arts*, vol. 1, no. 50, pp. 171–182, 2020.
- [21] S. A. Khan, S. B. Khan, A. Farooq, and A. M. Asiri, "A facile synthesis of CuAg nanoparticles on highly porous ZnO/carbon black-cellulose acetate sheets for nitroarene and azo dyes reduction/degradation," *International Journal of Biological Macromolecules*, vol. 130, pp. 288–299, 2019.
- [22] S. Nasiri Khalil Abad, M. Mozammel, J. Moghaddam, A. Mostafaei, and M. Chmielus, "Highly porous, flexible and robust cellulose acetate/Au/ZnO as a hybrid photocatalyst," *Applied Surface Science*, vol. 526, 2020.
- [23] M. A. Abu-Dalo, S. A. Al-Rosan, and B. A. Albiss, "Photocatalytic degradation of methylene blue using polymeric membranes based on cellulose acetate impregnated with zno nanostructures," *Polymers (Basel)*, vol. 13, no. 19, 2021.
- [24] M. P. Indumathi, K. Saral Sarojini, and G. R. Rajarajeswari, "Antimicrobial and biodegradable chitosan/cellulose acetate phthalate/ZnO nano composite films with optimal oxygen permeability and hydrophobicity for extending the shelf life of black grape fruits," *Int. J. Biol. Macromol.*, vol. 132, pp. 1112–1120, 2019.
- [25] W. D. Callister and D. G. Rethwisch, "Phase Transformations: Development of Microstructure and Alternation of Mechanical Properties," *Mater. Sci. Eng. An Introd.*, pp. 356–407, 2013.
- [26] M. T. Hayajneh, F. M. Al-Oqla, and M. M. Al-Shrida, "Hybrid green organic/inorganic filler polypropylene composites: Morphological study and mechanical performance investigations," *E-Polymers*, vol. 21, no. 1, pp. 710–721, 2021.
- [27] Y. Zare and K. Y. Rhee, "Analysis of critical interfacial shear strength between polymer matrix and carbon nanotubes and its impact on the tensile strength of nanocomposites," *Journal of Materials Research and Technology*, vol. 9, no. 3, pp. 4123–4132, 2020.
- [28] Q. A. Hamad, J. K. Oleiwi, and S. A. Abdulrahman, "Tensile properties of laminated composite prosthetic socket reinforced by different fibers," *Materials Today: Proceedings*. 2021.

- [29] C. O. Ndukwe, B. O. Ezurike, and P. C. Okpala, “Comparative studies of experimental and numerical evaluation of tensile properties of Glass Fibre Reinforced Polyester (GFRP) matrix,” *Heliyon*, vol. 7, no. 5, p. e06887, 2021.
- [30] T. Noguchi, M. Endo, K. Niihara and H. Jinnai, “Cellulose nanofiber-elastomer composites with high tensile strength, modulus, toughness, and thermal stability prepared by high-shear kneading,” *Composites Science and Technology*, vol. 188, 2020.
- [31] D. P. and S. K. Narayanankutty, “Styrenated phenol modified nanosilica for improved thermo-oxidative and mechanical properties of natural rubber,” *Polymer Testing*, vol. 82, 2020.
- [32] S. M. Gonçalves, D. C. dos Santos, J. F. G. Motta, R. R. dos Santos, D. W. H. Chávez, and N. R. de Melo, “Structure and functional properties of cellulose acetate films incorporated with glycerol,” *Carbohydr. Polym.*, vol. 209, no. January, pp. 190–197, 2019.
- [33] S. Naghibi, M. Gharagozlou, and S. Vahed, “Antibacterial response of Cd-TiO₂/PEG/folic acid nanocomposite under ultraviolet, visible light, or ultrasonic irradiation,” *J. Nanostructures*, vol. 9, no. 4, pp. 768–775, 2019.
- [34] P. Mehdizadeh and Z. Tavangar, “Photocatalyst Ag@N/TiO₂ nanoparticles: Fabrication, characterization, and investigation of the effect of coating on methyl orange dye degradation,” *J. Nanostructures*, vol. 7, no. 3, pp. 216–222, 2017.
- [35] L. Al-Naamani, S. Dobretsov, and J. Dutta, “Chitosan-zinc oxide nanoparticle composite coating for active food packaging applications,” *Innovative Food Science and Emerging Technologies*, vol. 38, pp. 231–237, 2016.
- [36] H. H. Bahjat, R. A. Ismail, G. M. Sulaiman, and M. S. Jabir, “Magnetic Field-Assisted Laser Ablation of Titanium Dioxide Nanoparticles in Water for Anti-Bacterial Applications,” *J. Inorg. Organomet. Polym. Mater.*, vol. 31, Sep. 2021.
- [37] M. A. Jihad, F. T. M. Noori, M. S. Jabir, S. Albukhaty, F. A. Almalki, and A. A. Alyamani, “Polyethylene glycol functionalized graphene oxide nanoparticles loaded with nigella sativa extract: A smart antibacterial therapeutic drug delivery system,” *Molecules*, vol. 26, no. 11, 2021.
- [38] S. Albukhaty, L. Albayati, H. Alkaragoly, and S. Al-Musawi, “Preparation and characterization of titanium dioxide nanoparticles and in vitro investigation of their cytotoxicity and antibacterial activity against *Staphylococcus aureus* and *Escherichia coli*,” *Anim. Biotechnol.*, Nov. 2020.
- [39] S. Albukhaty, H. Alkaragoly, and M. Dragh, “Synthesis of zinc oxide nanoparticles and evaluated its activity against bacterial isolates,” *J. Biotech Res.*, vol. 11, pp. 47–53, Jan. 2020.
- [40] Z. Khedaer, D. Ahmed, and S. Al-Jawad, “Investigation of Morphological, Optical, and Antibacterial Properties of Hybrid ZnO-MWCNT Prepared by Sol-gel,” *J. Appl. Sci. Nanotechnol.*, vol. 1, no. 2, pp. 66–77, 2021.
- [41] A. J. Haider, R. H. Al-Anbari, H. A. Mohammed and D. S. Ahmed, “Synthesis of Multi-Walled Carbon Nanotubes Decorated with Zinc Oxide Nanoparticles for Removal of Pathogenic Bacterial,” *Eng. Technol. J.*, vol. 36, no. 10A, 2018.
- [42] R. Saleh, O. Salman, and M. Dawood, “Physical Investigations of Titanium Dioxide Nanorods Film Prepared by Hydrothermal Technique,” *J. Appl. Sci. Nanotechnol.*, vol. 1, no. 3, pp. 32–41, 2021.
- [43] D. Hassan and M. Zayer, “Study and Investigation of the Effects of the OTA Technique on the Physical Properties of the ZnO Thin Films Prepared by PLD,” *J. Appl. Sci. Nanotechnol.*, vol. 1, no. 4, pp. 32–43, 2021.